VOL. 5, NO. 5, MAY 2010 ISSN 1819-6608
ARPN Journal of Engineering and Applied Sciences


www.arpnjournals.com

NUMERICAL SOLUTION OF LONGITUDINAL AND TORSIONAL OSCILLATIONS OF A CIRCULAR CYLINDER WITH SUCTION IN A COUPLE STRESS FLUID

J. V. Ramana Murthy, G. Nagaraju and P. Muthu
Department of Mathematics, National Institute of Technology, Warangal, A.P., India
E-Mail: jvrjosyula@yahoo.co.in

ABSTRACT

The flow of a couple stress fluid generated by performing longitudinal and torsional oscillations of a porous circular cylinder subjected to constant suction at the surface of the cylinder is studied. A finite difference method is proposed to analyze the velocity components, in an infinite expanse of an incompressible couple stress fluid under vanishing couple stresses of type A condition or super adherence condition of type B on the boundary. The effects of couple stress parameter, Reynolds number and the ratio of couple stress viscosities parameter on transverse and axial velocity components are studied. The drag force acting on the wall of the cylinder is derived and effects of couple stress parameters on drag are shown graphically.

Keywords: couple stress fluid, longitudinal and torsional oscillations, drag, suction, injection.

1. INTRODUCTION

In numerous technological applications, the fluids in use do not obey the commonly assumed linear relationship between the stress and the rate of strain at a point and their accurate flow behavior cannot be predicted by the classical Newtonian theory. Such fluids are recognized as non-Newtonian fluids. In particular, the interest in non-Newtonian fluids has grown considerably, due largely to the demand of such diverse areas as biorheology, geophysics and chemical and petroleum industries. For this reason several models have been proposed to predict the non-Newtonian behavior of various types of fluids. One class of fluids which has gained considerable attention in recent years is the couple stress fluid. Couple stresses are a consequence of the assumption that the interraction of one part of a body on another, across a surface, is equivalent to a force and moment distribution. Couple stress fluids consist of rigid, randomly oriented particles suspended in a viscous medium such as blood fluids, electro-rheological fluids and synthetic fluids. The main feature of couple stress fluid is that the stress tensor is anti-symmetric. Stokes [1] generalized the classical model to include the effect of the presence of the couple stresses and this couple stress model has been widely used because of its relative Mathematical simplicity compared with the other models developed for effects of the couple stresses. This fluid theory is discussed in detail by Stokes himself in his treatise "Theories of Fluids with Microstructure" [2] wherein he also presented a long list of problems discussed by researchers with reference to this theory. Recently, the study of couple stress fluid flows has been the subject of great interest, due to its widespread industrial and scientific applications in pumping fluids, such as synthetic fluids, polymer-thickened oils, liquid crystals and animal bloods. Other important fields where couple stress fluids have applications are squeezing and lubrication theory.

The motion of fluids through porous permeable surfaces at low Reynolds numbers has long been an important subject in the field of chemical, biomedical, and environmental engineering and science. This phenomenon is fundamental in nature and is of great practical importance in many diverse applications like production of oil and gas from geological structures, the gasification of coal, the retorting of shale oil, filtration, surface catalysis of chemical reactions, adsorption, coalescence, drying, ion exchange and chromatography.

Starting from Couette flows, the flow generated in fluids by the motion of surfaces have been attracting the researchers. Among them, the study of flow due to longitudinal and torsional oscillations presents some interest in different engineering areas like Oceanography, the technology of vibrations on machinery, the process of certain polymer liquid crystals, and the offshore drilling of oil. There are three physical situations in which the study of the longitudinal and torsional oscillations can be applied. The first application is in lubrication theory. The cylindrical bearings containing a non-Newtonian fluid lubricant are subject to longitudinal and torsional vibrations on the machinery. A second application is the flow of polymer liquid crystals made of dumbbell like molecules processed inside a circular cylinder which is subject to longitudinal and torsional oscillations. And finally, a possible third application is the flow of mud in the drillstring of an offshore oil drilling unit which is subjected to oscillations due to oceanic waves.

The motion of a classical viscous fluid due to the rotation of an infinite cylindrical rod immersed in the fluid was first described by Stokes [3]. Later following the work, many flow problems due to the motion of bodies were solved. Some flow problems related to the motion of a cylindrical rod performing longitudinal and torsional oscillations are given below. Casarella *et al*., [4] studied the external flow due to longitudinal and torsional oscillations of a rod in a Newtonian fluid and obtained an exact solution for the same. Rajagopal [5] studied the

same problem for the case of a second grade fluid. Ramkissoon and Majumdar [6] studied the internal flow due to longitudinal and torsional oscillations of a viscous fluid and they derived an analytical expression for velocities, shear stresses and drag on the cylinder. Ramkissoon *et al.,* [7] obtained an exact solution for an infinite rod undergoing both longitudinal and torsional oscillations in a polar fluid and they have presented the effect of micropolar parameters on the microrotation and velocity fields graphically. Calmelet-Eluhu *et al.,* [8] studied the internal flow of a micropolar fluid inside a circular cylinder subject to longitudinal and torsional oscillations and they have shown the effect of micropolar fluid on two components velocity field through graphs. Owen and Rahaman [9] studied the same type of flow with an Oldroyd-B liquid.

A large number of theoretical investigations dealing with steady incompressible laminar flow with either injection or suction at the boundaries have appeared during the last few decades. Several authors, to mention some [10-13] have studied the steady laminar flow of an incompressible viscous fluid in a two-dimensional channel with parallel porous walls. Soundalgekar *et al.,* [14] studied the effects of couple stresses on the oscillatory flow past porous, infinite, flat plate when the free stream velocity oscillates in magnitude about a constant mean. Eldabe *et al.,* [15] have studied the effect of couple stresses on an unsteady MHD Eyring Powell model of non-Newtonian fluid flow between two parallel fixed porous plates under a uniform external magnetic field. They have shown the effects of couple stress parameters and Hartmann number on velocity distributions through graphs. Dewakar *et al.,* [16] studied the Stokes' first and second problems for an incompressible couple stress fluid by using the condition that couple stresses vanish on the boundary. They have plotted the velocity profiles for different times and different values of couple stress Reynolds number. Srinivasacharya *et al.,* [17] studied the laminar flow of a couple stress fluid in a porous channel with expanding or contracting walls with symmetric injection or suction along the uniformly expanding porous walls by using similarity transformation. They have presented graphs for velocity components and temperature distribution for different values of the fluid and geometric properties. Ramana Murthy *et al.,* [18] studied the steady MHD flow of a micropolar fluid through a porous circular pipe with constant suction/injection. They have shown the effects of skin friction with respect to micropolar parameters and Hartmann number through graphs. To the extent of the knowledge of the authors, very few literatures are available on the flow due to oscillations of a rod in couple stress fluids. The problems mentioned in [7] and [8] are some examples in this direction. Hence, in this paper we consider the flow of couple stress fluid generated by a porous circular cylinder performing longitudinal and torsional oscillations and subjected to suction velocity at the surface.

2. FORMULATION OF THE PROBLEM

Consider a porous circular cylinder of radius '*a*' in an infinite expansion of a couple stress fluid. The cylinder is subjected to torsional oscillations, Exp ($i\omega_1 t$) and longitudinal oscillations, Exp ($i\omega_2 t$) with amplitudes $q_0 \sin\beta_0$, $q_0 \cos\beta_0$ along the respective directions where ω_1 is the frequency of the torsional oscillations, ω_2 is the frequency of the longitudinal oscillations, q_0 is the magnitude of the oscillations and β_0 is the angle between the direction of torsional oscillations and the base vector e_0. i.e., the cylinder oscillates with velocity as given by the expression

$$\boldsymbol{Q}_{\Gamma} = q_0 \left(Sin\,\beta_0 e^{i\omega_1 \tau}\, \boldsymbol{e}_{\theta} + Cos\,\beta_0 e^{i\omega_2 \tau}\, \boldsymbol{e}_{z} \right).$$

u_0 is a suction or injection velocity on the surface of the porous cylinder. Cylindrical polar coordinate system is considered with the Z-axis along the axis of the cylinder and origin on the axis. Let R, θ and Z denote the radial, azimuthal and axial coordinates respectively of a point in the region of flow. Now we consider the flow generated in the couple stress fluid due to the oscillations of the cylinder. The physical model illustrating the problem under consideration is shown in Figure-1.

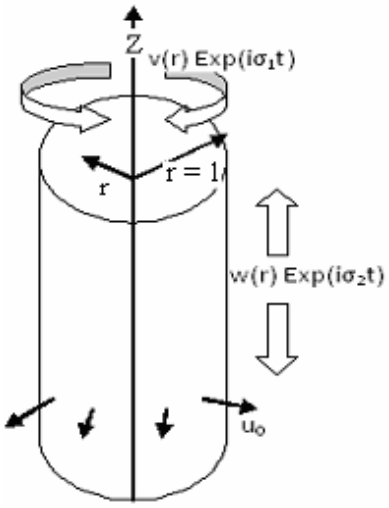

Figure-1. Geometrical representation of the problem: non-dimensional form.

After neglecting body forces and body couples, the condition of incompressibility and the equation motion for a couple stress fluid, as given by Stokes [1] are:

$$\nabla_1 \cdot \boldsymbol{Q} = 0 \quad (1)$$

$$\rho\left(\frac{\partial \boldsymbol{Q}}{\partial \tau} + \boldsymbol{Q}\cdot\nabla_1 \boldsymbol{Q}\right) = -\nabla_1 \boldsymbol{P} - \mu\ \nabla_1 \times \nabla_1 \times \boldsymbol{Q} - \eta\ \nabla_1 \times \nabla_1 \times \nabla_1 \times \nabla_1 \times \boldsymbol{Q} \quad (2)$$

Where $\boldsymbol{Q}$ is velocity vector, $\boldsymbol{P}$ is fluid pressure, ρ is density, τ is time, μ is viscosity and η is couple stress viscosity coefficients, ∇_1 is the dimensional gradient. By

nature of the flow, the velocity components are axially symmetric and depend only on radial distance and time. Hence the velocity vector is taken of the form

$$\boldsymbol{Q} = U(R)\,\boldsymbol{e}_r + V(R,\tau)\,\boldsymbol{e}_\theta + W(R,\tau)\,\boldsymbol{e}_z \qquad (3)$$

Let us introduce the following non dimensional scheme

$$\sigma_1 = \frac{\omega_1 a}{q_0}, \sigma_2 = \frac{\omega_2 a}{q_0}, r = \frac{R}{a}, \boldsymbol{q} = \frac{\boldsymbol{Q}}{q_0}, p = \frac{P}{\rho q_0^2},$$

$$t = \frac{q_0}{a}\tau,\ n_1 = \frac{u_0}{q_0},\ u = \frac{U}{q_0},\ v = \frac{V}{q_0},\ w = \frac{W}{q_0} \qquad (4)$$

By the non-dimensional scheme (4) in (1) and (2), the equations for the flow are transformed to the following non-dimensional form.

$$\nabla . \boldsymbol{q} = 0 \qquad (5)$$

$$Re\left(\frac{\partial \boldsymbol{q}}{\partial t} + \boldsymbol{q}.\nabla \boldsymbol{q}\right) = -Re\,\nabla \boldsymbol{p} - \nabla \times \nabla \times \boldsymbol{q} - S\,\nabla \times \nabla \times \nabla \times \nabla \times \boldsymbol{q} \qquad (6)$$

where $Re = \frac{\rho q_0 a}{\mu}$ = Reynolds number and $S = \frac{\eta}{\mu a^2}$ = couple stress parameter.

Now to match with the oscillating boundary, the velocity in (3) is assumed in the form

$$\boldsymbol{q} = u(r)\boldsymbol{e}_r + v(r)\,e^{i\sigma_1 t}\,\boldsymbol{e}_\theta + w(r)e^{i\sigma_2 t}\,\boldsymbol{e}_z \qquad (7)$$

The equation (6) will give raise to the following three scalar equations in the directions of base vectors

$$\frac{dp}{dr} = \frac{n_1^2}{r^3} + \frac{v^2}{r}e^{2i\sigma_1 t} \qquad (8)$$

$$Re\left(i\sigma_1 v + \frac{n_1}{r}\left(v' + \frac{v}{r}\right)\right) = -S\,D^4 v + D^2 v \qquad (9)$$

$$Re\left(i\sigma_2 w + \frac{n_1}{r}w'\right) = \left(\frac{1}{r}w' + w''\right) - S\left(w^{iv} + \frac{2}{r}w''' - \frac{1}{r^2}w'' + \frac{1}{r^3}w'\right) \qquad (10)$$

where

$$D^2 v = v'' + \frac{1}{r}v' - \frac{1}{r^2}v \quad \text{and}$$

$$D^4 v = v^{iv} + \frac{2}{r}v''' - \frac{3}{r^2}v'' + \frac{3}{r^3}v' - \frac{3}{r^4}v$$

Using D^2v and D^4v in the equation (9), we get

$$v^{iv} + \frac{2}{r}v''' + \left(\boldsymbol{a}_1 - \frac{3}{r^2}\right)v'' + \left(\frac{\boldsymbol{a}_2}{r} + \frac{3}{r^3}\right)v' + \left(\boldsymbol{a}_3 + \frac{\boldsymbol{a}_4}{r^2} - \frac{3}{r^4}\right)v = 0 \qquad (11)$$

where

$$a_1 = -\frac{1}{S}, a_2 = \frac{Re\,n_1 - 1}{S}, a_3 = \frac{Re\,i\,\sigma_1}{S} \text{ and } a_4 = \frac{Ren_1 + 1}{S}$$

Similarly we write (10) as

$$w^{iv} + \frac{2}{r}w''' + \left(b_1 - \frac{1}{r^2}\right)w'' + \left(\frac{b_2}{r} + \frac{1}{r^3}\right)w' + b_3\,w = 0 \qquad (12)$$

where

$$b_1 = -\frac{1}{S},\ b_2 = \frac{Ren_1 - 1}{S} \text{ and } b_3 = \frac{Rei\sigma_2}{S}$$

Now the equations (11) and (12) are solved for v and w under the no slip condition and type A condition or type B condition on the boundary. These conditions are given as follows.

3. BOUNDARY CONDITIONS

No slip condition

The velocity of the fluid on the boundary is equal to the velocity of the boundary. It is explicitly given by

$\boldsymbol{Q}_\Gamma$ = Velocity of Γ =

$$q_0\left(cos\,\beta_0 e^{i\omega_1 \tau}\,\boldsymbol{e}_\theta + sin\,\beta_0 e^{i\omega_2 \tau}\,\boldsymbol{e}_z\right)$$

It takes the following in non-dimensional form

$$\boldsymbol{q}\,|_{r=1} = cos\,\beta_0 e^{i\sigma_1 t}\,\boldsymbol{e}_\theta + sin\,\beta_0 e^{i\sigma_2 t}\,\boldsymbol{e}_z$$

This condition can be explicitly written as in the following equations

$$v(1) = cos\beta_0 \text{ And } w(1) = sin\beta_0 \qquad (13)$$

Type A condition

Type A-condition represents vanishing of couple stress tensor on the boundary. The constitutive equation for couple stress tensor $\boldsymbol{M}$ is given by

$$\boldsymbol{M} = mI + 2\eta\,\nabla_1(\nabla_1 \times \boldsymbol{Q}) + 2\eta'\,[\nabla_1(\nabla_1 \times \boldsymbol{Q})]^T \qquad (14)$$

Taking

$$\nabla \times \boldsymbol{q} = -w'\,e^{i\sigma_2 t}\,\boldsymbol{e}_\theta + \left(v' + \frac{v}{r}\right)e^{i\sigma_1 t}\,\boldsymbol{e}_z$$ in the equation (14), we get the expression for $\boldsymbol{M}$ as

$$\boldsymbol{M} = m\left(\boldsymbol{e}_r\boldsymbol{e}_r + \boldsymbol{e}_\theta\boldsymbol{e}_\theta + \boldsymbol{e}_z\boldsymbol{e}_z\right) + \left(-\frac{2\eta\,q_0}{\boldsymbol{a}^2}w'' + \frac{2\eta' q_0}{\boldsymbol{a}^2}\frac{1}{r}w'\right)e^{i\sigma_2 t}\,\boldsymbol{e}_r\boldsymbol{e}_\theta + \left(-\frac{2\eta' q_0}{\boldsymbol{a}^2}w'' + \frac{2\eta\,q_0}{\boldsymbol{a}^2}\frac{1}{r}w'\right)e^{i\sigma_2 t}\,\boldsymbol{e}_\theta\boldsymbol{e}_r$$

$$+\frac{2\eta\, q_0}{a^2}\, D^2 v\; e^{i\sigma_1 t}\, \boldsymbol{e}_r \boldsymbol{e}_z + \frac{2\eta' q_0}{a^2}\, D^2 v\, e^{i\sigma_1 t}\, \boldsymbol{e}_z \boldsymbol{e}_r$$

If $\boldsymbol{M}$ vanishes on the boundary, we get the conditions that

$$D^2 v = 0 \text{ and } w'' - e\frac{1}{r}w' = 0 \text{ where } e = \frac{\eta'}{\eta} \text{ on } r = 1 \qquad (15)$$

Type B condition

Type B-condition is the super adherence condition on the boundary. This condition requires that angular velocity of the fluid particle on the boundary is equal to angular velocity of the boundary. i.e., $\boldsymbol{\omega}_\Gamma = \frac{1}{2}\nabla_1 \times \boldsymbol{Q}_\Gamma$ this implies that

$$w'\big|_{r=1} = -2\sigma_1 \text{ And } \frac{d}{dr}(r v)\Big|_{r=1} = 0 \qquad (16)$$

As $r \to \infty$, the fluid is at rest and boundary conditions can be taken as

$$v = w = D^2 v = {}_{w'' - e\frac{1}{r}w' = 0} = \frac{d}{dr}(r v) = 0 \quad on \quad r = \infty \qquad (17)$$

4. FINITE DIFFERENCE METHOD OF SOLUTION

In view of the complicated nature of two equations (11) and (12), the analytical solution for v and w seems to be beyond reach. The details of finite difference method used here can be studied from Ref. [19], for obtaining the solution for v and w. We take 50 units of distance from origin is very large representing infinity. Hence we discretise the interval [1, 50] into n subintervals with n+ 1 node. Each node is represented by $r_i = 1 + i\,h$, with $h = 49/n$ the step length, starting from first node $r_0 = 1$ to the last node $r_n = 50$. The values of the functions v, w at r_i are given by v_i and w_i. The symmetric derivative formulae at the i'th node are given as below:

$$\left.\begin{aligned} v_i' &= \frac{v_{i+1} - v_{i-1}}{2h} \\ v_i'' &= \frac{v_{i+1} - 2v_i + v_{i-1}}{h^2} \\ v_i''' &= \frac{v_{i+2} - 2v_{i+1} + 2v_{i-1} - v_{i-2}}{2h^3} \\ v_i^{iv} &= \frac{v_{i+2} - 4v_{i+1} + 6v_i - 4v_{i-1} + v_{i-2}}{h^4} \end{aligned}\right\} \qquad (18)$$

Substituting these derivatives given in (18), in the equation (11) we get

$$t_{1,i}\, v_{i-2} + t_{2,i}\, v_{i-1} + t_{3,i}\, v_i + t_{4,i}\, v_{i+1} + t_{5,i}\, v_{i+2} = 0 \qquad (19)$$

where

$$t_{1,i} = r_i^4 - h\, r_i^3$$

$$t_{2,i} = -4 r_i^4 + 2h\, r_i^3 + h^2\left(\boldsymbol{a}_1 r_i^4 - 3 r_i^2\right) - \left(\boldsymbol{a}_2 r_i^3 + 3 r_i\right)\frac{h^3}{2}$$

$$t_{3,i} = 6 r_i^4 - 2h^2\left(\boldsymbol{a}_1 r_i^4 - 3 r_i^2\right) + \left(\boldsymbol{a}_3 r_i^4 + \boldsymbol{a}_4 r_i^2 - 3\right)h^4$$

$$t_{4,i} = -4 r_i^4 - 2 r_i^3\, h + h^2\left(\boldsymbol{a}_1 r_i^4 - 3 r_i^2\right) + \left(\boldsymbol{a}_2 r_i^3 + 3 r_i\right)\frac{h^3}{2}$$

$$t_{5,i} = r_i^4 + h\, r_i^3 \qquad (20)$$

The finite difference form of (12) is as the following:

$$s_{1,i}\, w_{i-2} + s_{2,i}\, w_{i-1} + s_{3,i}\, w_i + s_{4,i}\, w_{i+1} + s_{5,i}\, w_{i+2} = 0 \qquad (21)$$

$$s_{1,i} = r_i^4 - h\, r_i^3$$

$$s_{2,i} = -4 r_i^4 + 2h\, r_i^3 + h^2\left(\boldsymbol{b}_1 r_i^4 - r_i^2\right) - \left(\boldsymbol{b}_2 r_i^3 + r_i\right)\frac{h^3}{2}$$

$$s_{3,i} = 6 r_i^4 - 2h^2\left(\boldsymbol{b}_1 r_i^4 - r_i^2\right) + \boldsymbol{b}_3 r_i^4 \boldsymbol{h}^4$$

$$s_{4,i} = -4 r_i^4 - 2 r_i^3\, h + h^2\left(\boldsymbol{b}_1 r_i^4 - r_i^2\right) + \left(b_2 r_i^3 + r_i\right)\frac{h^3}{2}$$

$$s_{5,i} = r_i^4 + h\, r_i^3 \qquad (22)$$

Type A solution for velocities *v* and *w*

We take the following boundary conditions

$$v_0 = v(1) = cos\beta_0 = n_2, \quad v_n = 0,$$

$$D^2 v\big|_{r=1} = 0 \text{ and } D^2 v\big|_{r=\infty} = 0 \qquad (23)$$

Evaluating (19) for different values of i we obtain

i = 0:

$$t_{1,0}\, v_{-2} + t_{2,0}\, v_{-1} + t_{4,0}\, v_1 + t_{5,0}\, v_2 = -t_{3,0}\, v_0$$

i = 1:

$$t_{1,1}\, v_{-1} + t_{3,1}\, v_1 + t_{4,1}\, v_2 + t_{5,1}\, v_3 = -t_{2,1}\, v_0$$

i = 2:

$t_{2,2}\, v_1 + t_{3,2}\, v_2 + t_{4,2}\, v_3 + t_{5,2}\, v_4 = -t_{1,2}\, v_0$

i = 3:

$t_{1,3}\, v_1 + t_{2,3}\, v_2 + t_{3,3}\, v_3 + t_{4,3}\, v_4 + t_{5,3}\, v_5 = 0$

…

i = n–1:

$t_{1,n-1}\, v_{n-3} + t_{2,n-1}\, v_{n-2} + t_{3,n-1}\, v_{n-1} + t_{5,n-1} v_{n+1} = -t_{4,n-1}\, v_n$

i = n:

$t_{1,n}\, v_{n-2} + t_{2,n}\, v_{n-1} + t_{4,n}\, v_{n+1} + t_{5,n-1}\, v_{n+2} = -t_{3,n}\, v_n$ (24)

Thus the system of equations (24) represents n+ 1 equation in n+3 unknowns. Hence we require two more equations. These can be obtained from

$$D^2 v\big|_{r=1} = 0 \text{ And } D^2 v\big|_{r=\infty} = 0 \quad (25)$$

Using the boundary conditions (25), then we have

$$t_1\, v_{-1} + t_2\, v_1 = t_3\, v_0 \text{ and } t_4\, v_{n-1} + t_5\, v_{n+1} = t_6\, v_n \quad (26)$$

Where

$$t_1 = r_0^2 - \frac{h\, r_0}{2},\ t_2 = r_0^2 + \frac{h\, r_0}{2},\ t_3 = 2\, r_0^2 + h^2,$$

$$t_4 = r_n^2 - \frac{h\, r_n}{2},\ t_5 = r_n^2 + \frac{h\, r_n}{2} \text{ and } t_6 = 2\, r_n^2 + h^2$$

Expressing the equations (24) and (26) in matrix form as

$$A_1 X_1 = B_1 \quad (27)$$

where the matrices A_1, X_1 and B_1 are given in the appendix. B_1 contains v_0 and v_n which are the value of v on the boundary and X_1 consists of values of v in the region. Solving the system (27) we get the solution for v.

Now we find solution for w by applying the boundary conditions

$$w_0 = w(1) = sin\beta_0 = \sqrt{1-n_2^2} = n_3,\ w_n = 0,$$

$$w'' - e\frac{1}{r}w'\Big|_{r=1} = 0 \text{ and } w'' - e\frac{1}{r}w'\Big|_{r=\infty} = 0 \quad (28)$$

Evaluating (21) for different values of i we obtain

i = 0:

$s_{1,0}\, w_{-2} + s_{2,0}\, w_{-1} + s_{4,0}\, w_1 + s_{5,0}\, w_2 = -s_{3,0}\, w_0$

i = 1:

$s_{1,1}\, w_{-1} + s_{3,1}\, w_1 + s_{4,1}\, w_2 + s_{5,1}\, w_3 = -s_{2,1}\, w_0$

i = 2:

$s_{2,2}\, w_1 + s_{3,2}\, w_2 + s_{4,2}\, w_3 + s_{5,2}\, w_4 = -s_{1,2}\, w_0$

i = 3:

$s_{1,3}\, w_1 + s_{2,3}\, w_2 + s_{3,3}\, w_3 + s_{4,3}\, w_4 + s_{5,3}\, w_5 = 0$

…

i = n–1:

$s_{1,n-1}\, w_{n-3} + s_{2,n-1}\, w_{n-2} + s_{3,n-1}\, w_{n-1} + s_{5,n-1}\, w_{n+1} = -s_{4,n-1}\, w_n$

i = n:

$s_{1,n}\, w_{n-2} + s_{2,n}\, w_{n-1} + s_{4,n}\, w_{n+1} + s_{5,n-1}\, w_{n+2} = -s_{3,n}\, w_n$ (29)

Thus the system of equations (29) represents n+1 equation in n+3 unknowns. Hence we require two more equations which are obtained from the boundary conditions

$$w'' - e\frac{1}{r}w'\Big|_{r=1} = 0 \text{ and } w'' - e\frac{1}{r}w'\Big|_{r=\infty} = 0,$$

then we have

$s_1\, w_{-1} + s_2\, w_1 = 2\, r_0\, w_0$ and

$s_3\, w_{n-1} + s_4\, w_{n+1} = 2\, r_n w_n$ (30)

Where $s_1 = r_0 + \frac{e\,h}{2}$, $s_2 = r_0 - \frac{e\,h}{2}$,

$s_3 = r_n + \frac{e\,h}{2}$ and $s_4 = r_n - \frac{e\,h}{2}$

Expressing the equations (29)-(30) in matrix form as

$$A_2 X_2 = B_2 \quad (31)$$

where the matrices A_2, X_2 and B_2 are given in the appendix. B_2 contains w_0 and w_n which are the value of w on the boundary and X_2 consists of values of w in the region. Solving the system (31) we get the solution for w

Type B solution for velocities *v* and *w*

We take the following boundary conditions

$v_0 = v(1) = cos\beta_0 = n_2$, $v_n = 0$, $\frac{d}{dr}(rv)\Big|_{r=1} = 0$ and

$\frac{d}{dr}(rv)\Big|_{r=\infty} = 0$

Using the boundary conditions $\frac{d}{dr}(rv)\Big|_{r=1} = 0$

and $\frac{d}{dr}(rv)\Big|_{r=\infty} = 0$, we get

$$v_{-1} - v_1 = \frac{2h}{r_0} v_0 \quad \text{And} \quad v_{n-1} - v_{n+1} = \frac{2h}{r_n}\, v_n \quad (32)$$

From (19) substituting i = 0, 1, 2…..n–1, n and from (32), writing in matrix we get as

$$A_3 X_1 = B_3 \quad (33)$$

where A_3, B_3 are given in appendix.

Similarly we use the following boundary conditions for velocity w as

$$w_0 = w(1) = sinb = \sqrt{1-n_2^2} = n_3 \ , \ w_n = 0,$$
$$w'|_{r=1} = -2\sigma_1 \text{ and } w'|_{r=\infty} = 0$$

Using the conditions $w'|_{r=1} = -2\sigma_1$ and $w'|_{r=\infty} = 0$, we get

$$w_{-1} - w_1 = 4\sigma_1 h \text{ and } w_{n-1} - w_{n+1} = 0 \quad (34)$$

From (21) substituting i = 0, 1, 2…..n–1, n and from (34), writing in matrix we get as

$$A_4 X_2 = B_4 \quad (35)$$

where A_4 and B_4 are given in the appendix. On solving (35), we get the solution for X_2, the values of axial velocity w .

5. DRAG ON THE CYLINDER

The drag D acting on a cylinder of length L is given by

$$D = \boldsymbol{a} L \int_0^{2\pi} \left(T_{21} cos\ \beta_0 + T_{31} sin\ \beta_0\right) d\theta \quad (36)$$

The stress component in (36) and Couple stress tensor $\boldsymbol{M}$ are defined by the following constitutive equation for couple stress fluids (Stokes [1]).

$$T_{ij} = -PI + \lambda\left(\nabla_1 \cdot \mathbf{Q}\right) I + \mu\left(\nabla_1 \mathbf{Q} + \left(\nabla_1 \mathbf{Q}\right)^T\right) + \frac{1}{2} I \times \left(\nabla_1 \cdot \boldsymbol{M}\right) \quad (37)$$

$$\boldsymbol{M} = mI + 2\eta \nabla_1\left(\nabla_1 \times \mathbf{Q}\right) + 2\eta'\left[\nabla_1\left(\nabla_1 \times \mathbf{Q}\right)\right]^T \quad (38)$$

The stress components T_{31} and T_{21} on the cylinder can be calculated as

$$T_{31} = \frac{\mu q_0}{\boldsymbol{a}}\left[w' + S\left(w''' + \frac{1}{r} w' - \frac{1}{r^2} w\right)\right] e^{i\sigma_2 t} \quad (39)$$

$$T_{21} = \frac{\mu q_0}{\boldsymbol{a}}\left[v' - \frac{v}{r} + S\left(v''' + \frac{2}{r} v'' - \frac{1}{r^2} v' + \frac{1}{r^3} v\right)\right] e^{i\sigma_1 t} \quad (40)$$

Applying the finite difference scheme for (39) and (40), the non-dimensional form of stress components are calculated as

$$T_{31} = \frac{\mu q_0}{\boldsymbol{a}\boldsymbol{h}^3}\left[-\frac{S}{2} w_{-2} + \left(\frac{-\boldsymbol{h}^2}{2} + S + \frac{Sh}{r_0} + \frac{Sh^2}{2r_0^2}\right) w_{-1} - \frac{2Sh}{r_0} w_0 + \left(\frac{h^2}{2} - S + \frac{Sh}{r_0} - \frac{Sh^2}{2r_0^2}\right) w_1 + \frac{S}{2} w_2\right] e^{i\sigma_2 t}$$

$$T_{21} = e^{i\sigma_1 t} \frac{\mu q_0}{\boldsymbol{a}\boldsymbol{h}^3}\left[-\frac{S}{2} v_{-2} + \left(\frac{-h^2}{2} + S + \frac{2Sh}{r_0} + \frac{Sh^2}{2r_0^2}\right) v_{-1} + \left(\frac{Sh^3}{r_0^3} - \frac{h^3}{r_0} - \frac{4Sh}{r_0}\right) v_0 + \left(\frac{h^2}{2} - S + \frac{2Sh}{r_0} - \frac{Sh^2}{2r_0^2}\right) v_1 + \frac{S}{2} v_2\right]$$

The non-dimensional drag can be calculated from (36) as

$$D' = T_{31}\ cos\ \beta_0 + T_{21}\ sin\ \beta_0 \quad (41)$$

Where $D' = \dfrac{Dh^3}{2L\pi\mu\, q_0}$

6. RESULTS AND DISCUSSIONS

The analytical expressions for the non-dimensional velocity components v, w and drag are given by the equations (11), (12) and (41) respectively. These values depend on the values of β_0, if $\beta_0 = 0$, we get only torsional oscillations and if $\beta_0 = \pi/2$, we get only axial (Longitudinal) oscillations.

The numerical results are presented in the form of graphs for S =10, Re=0.1, σ_1=0.25, σ_2=0.5, β_0=0.7, $n1$=0.6, $t=\pi$. The Figures for type A boundary condition are shown on left column and the Figures for type B conditions are on the right column. The velocities v and w at different Reynolds number with type A and type B boundary conditions are shown in Figures 2-5. We notice that as Reynolds number Re increases both the velocities v and w decrease. The velocities v and w at different non-dimensional times are shown in Figures 6-9. We observe that the transverse and axial velocity components near the cylinder are developing and fluctuating around zero with the same frequency as the cylinder. At the start of a cycle, the flow has its maximum velocities located at the surface of cylinder, with a gradual decrease toward zero in the region away from the cylinder. As the cycle continues, the velocities decrease with the maximum values no longer at the cylinder surface but inside the flow field. From Figures 10-13, we see that as the couple stress parameter S increases, the transverse velocity v decrease for type A condition and increases for type B condition and the axial velocity w increases for type A condition, while it decreases for type B condition. Type B boundary condition doesn't involve the parameter e, which is the ratio of couple stress viscosity coefficients η and η'. In

type A condition, as it can be seen from Figures 14-15 both the axial and transverse velocities are insignificant with *e*.

The non-dimensional drag is calculated numerically for different values of non-dimensional time in multiples of π/σ_2 at fixed values of σ_1, σ_2 and the results are shown in the Figures 16-17. In the equations of motion, local acceleration term dominates if σ_1, σ_2 are large. To have all terms of LHS in the same order in equations (9) and (10), the frequency parameters σ_1, σ_2 are to be small. Hence we take both $|\sigma_1|$, $|\sigma_2| < 1$. In the calculation of drag also we observe that if $|\sigma_1|<1$, $|\sigma_2| < 1$, the drag will be within reasonable values. From Figures 16-17, it can be seen that as the couple stress parameter S increases, the amplitude of oscillations for drag increases for both the type A and type B conditions. It can be seen for both the type A and type B conditions as σ_1 increase, the variation in drag at the cylinder wall are changing in amplitude and frequency (Figures 18-19). From Figure-20 and Figure-21, it is observed that the drag is insignificant to the variations in σ_2 for type a condition and for type B condition the drag oscillates irregularly as σ_2 increases. From Figures 22-23, we note that as Reynolds number *Re* increases magnitude of drag increases for small values of suction; but for higher values of suction drag increases for small values of Reynolds number and then decreases at higher values and almost constant for very high values of suction rate. From Figure-24, we note that drag is insignificant to the variation in e, for type a condition and type B condition is independent of e.

7. CONCLUSIONS

We have observed that:

i. The flow is sensitive with respect to couple stress parameter *S* and type A and type B conditions show opposite trend. i.e., the transverse velocity v decreases for type A condition, it increases for type B condition;
ii. The drag increases as S increases i.e. the drag offered by viscous fluids is less than that of couple stress fluids; and
iii. Suction on the cylinder decreases the drag.

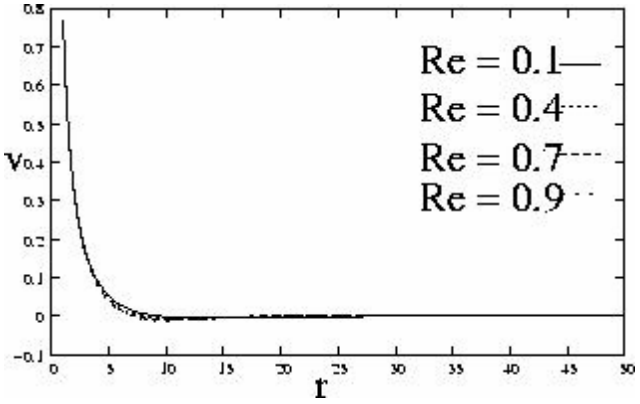

Figure-2. Type A variation of *v* with *r*.

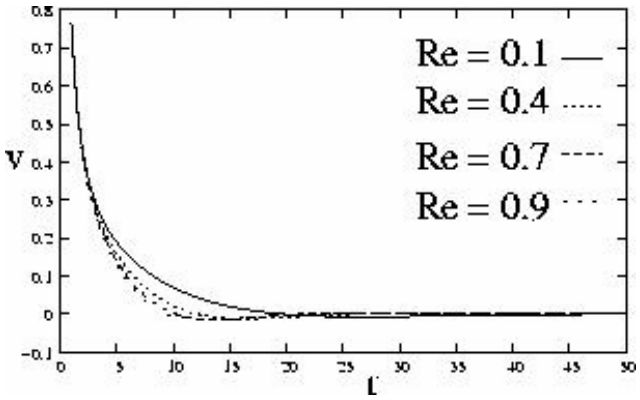

Figure-3. Type B variation of *v* with *r*.

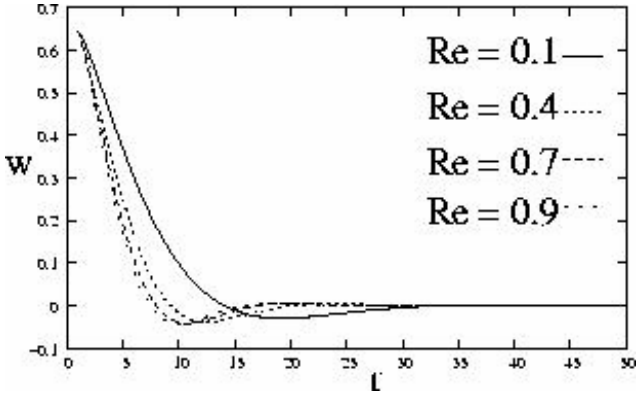

Figure-4. Type A variation of *w* with *r*.

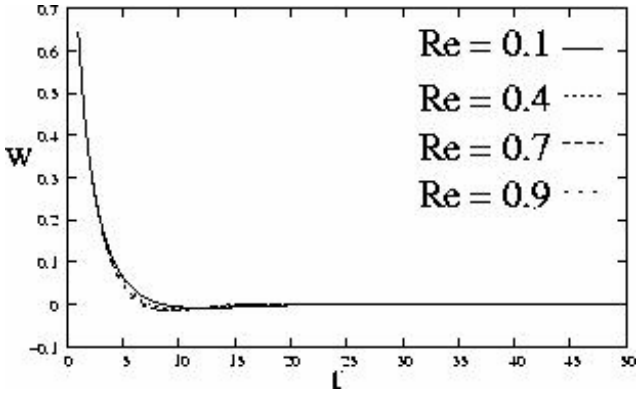

Figure-5. Type B variation of *w* with *r*.

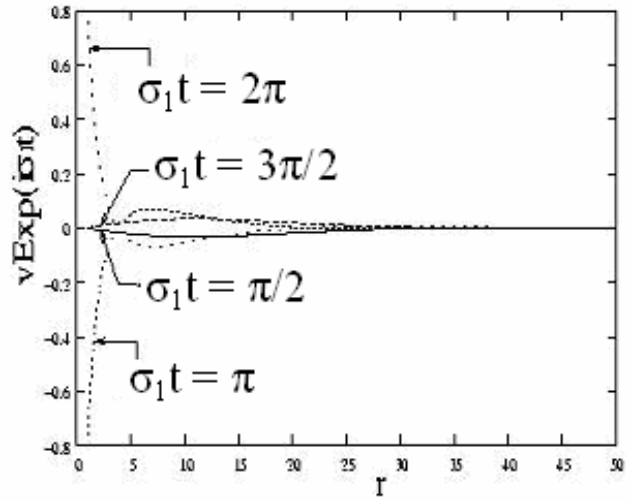

Figure-6. Type A variation of $vE\exp(i\sigma_1 t)$ with r.

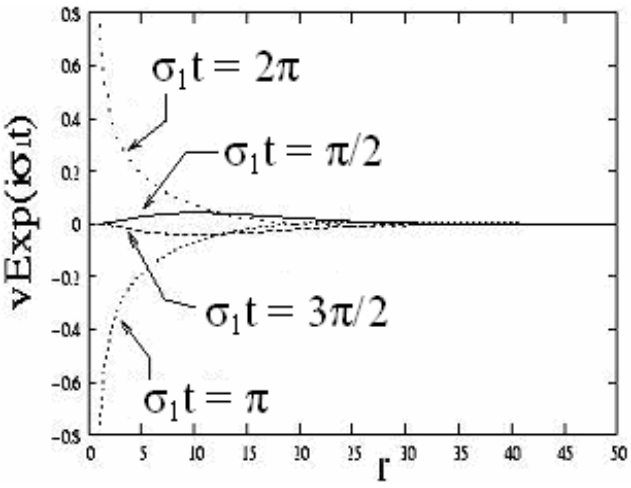

Figure-7. Type B variation of $v\,E\exp(i\sigma_1 t)$ with r.

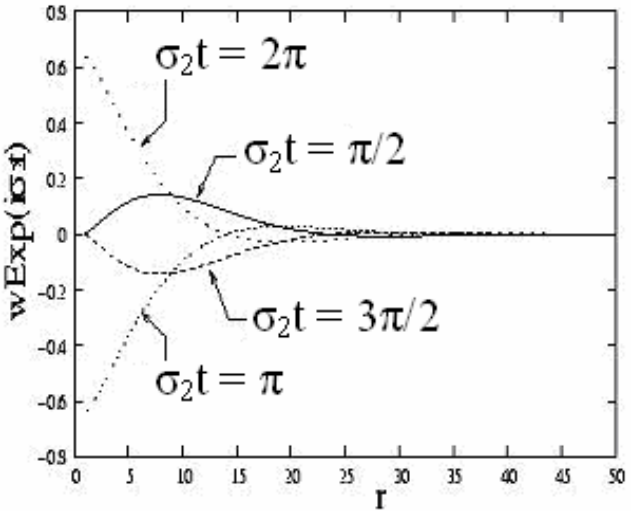

Figure-8. Type A variation of $w\,E\exp(i\sigma_2 t)$ with r.

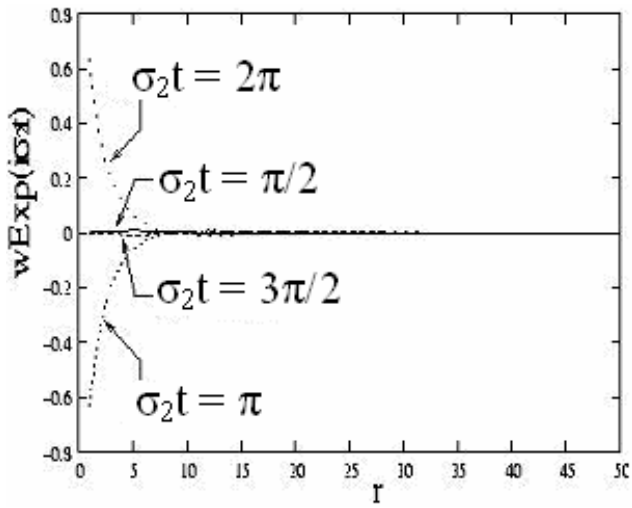

Figure-9. Type B variation of $w\,E\exp(i\sigma_2 t)$ with r

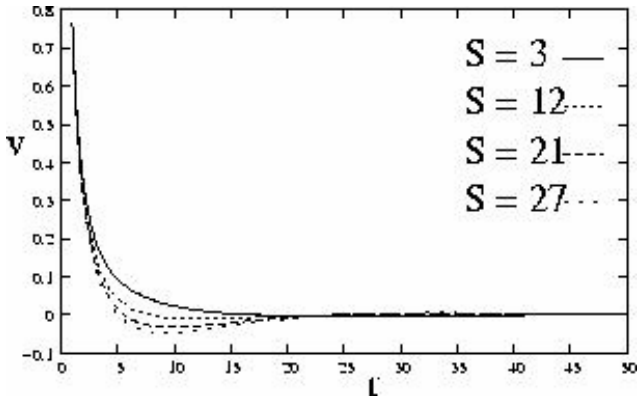

Figure-10. Type A variation of v with r.

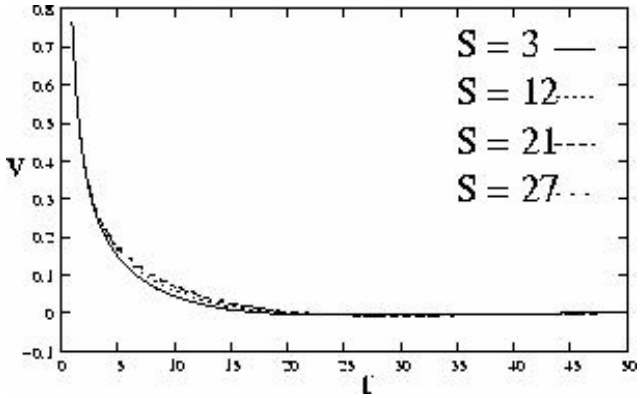

Figure-11. Type B variation of v with r.

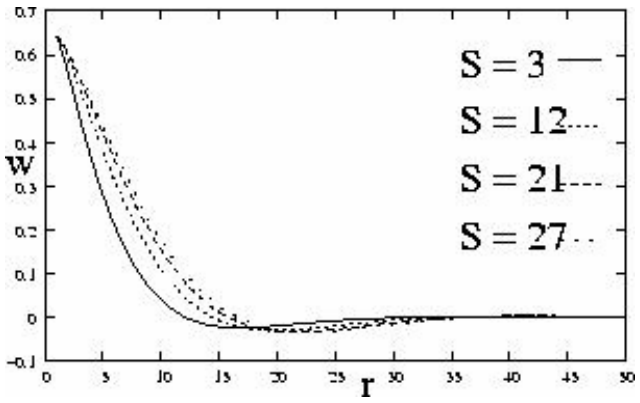

Figure-12. Type A variation of *w* with *r*.

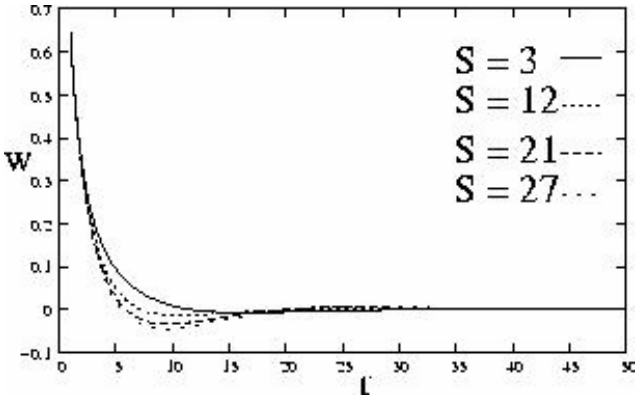

Figure-13. Type B variation of *w* with *r*.

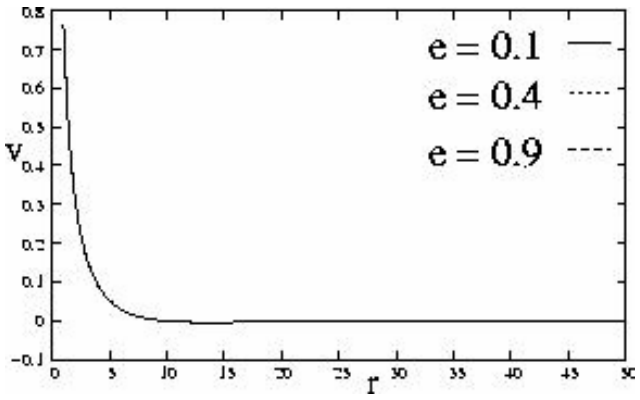

Figure-14. Type A variation of *v* with *r*.

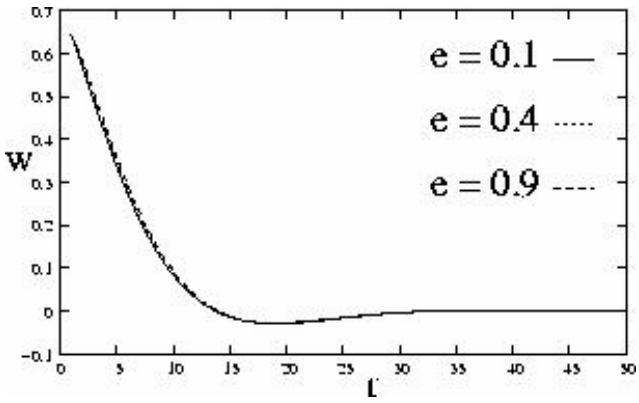

Figure-15. Type A variation of *w* with *r*.

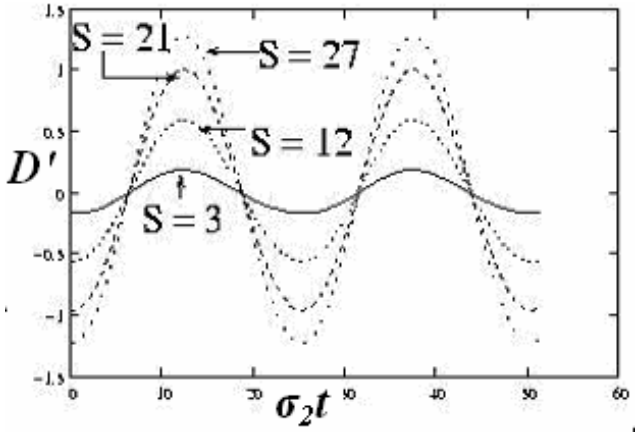

Figure-16. Type A variation of *D′* with $\sigma_2 t$.

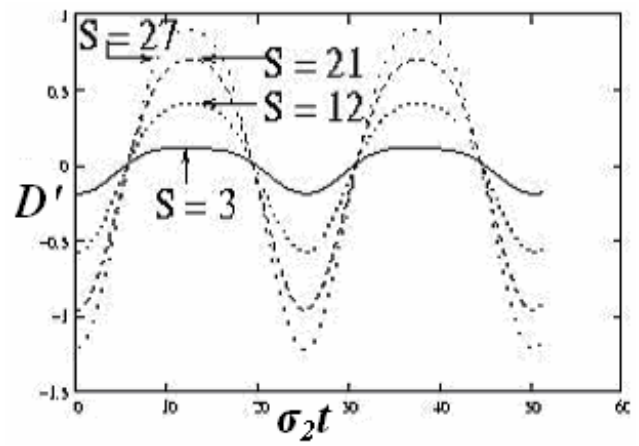

Figure-17. Type B variation of *D′* with $\sigma_2 t$.

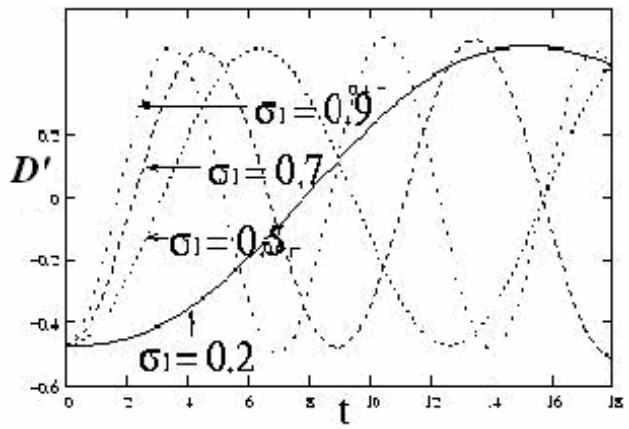

Figure-18. Type A variation of D' with t.

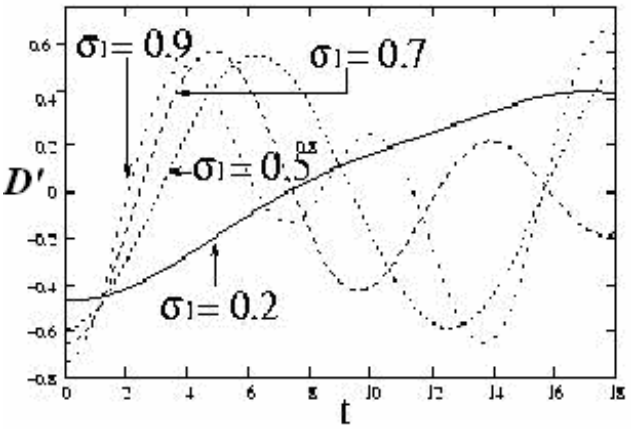

Figure-19. Type B variation of D' with t.

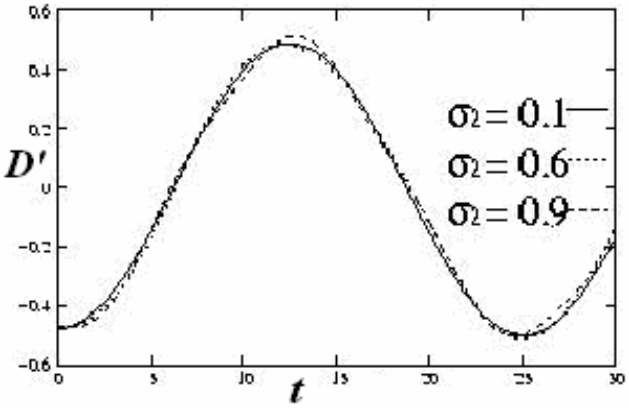

Figure-20. Type A variation of D' with t.

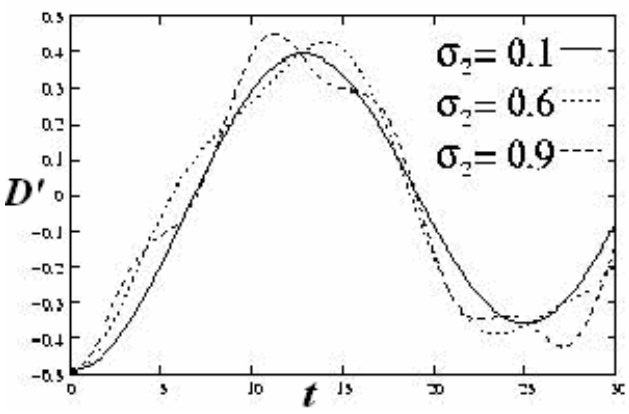

Figure-21. Type B variation of D' with t.

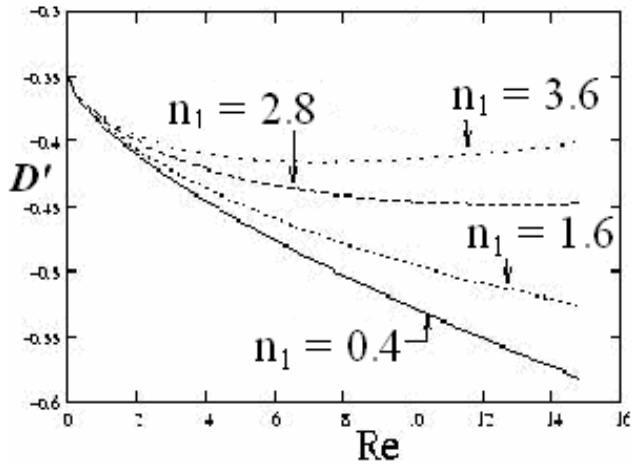

Figure-22. Type A variation of D' with Re.

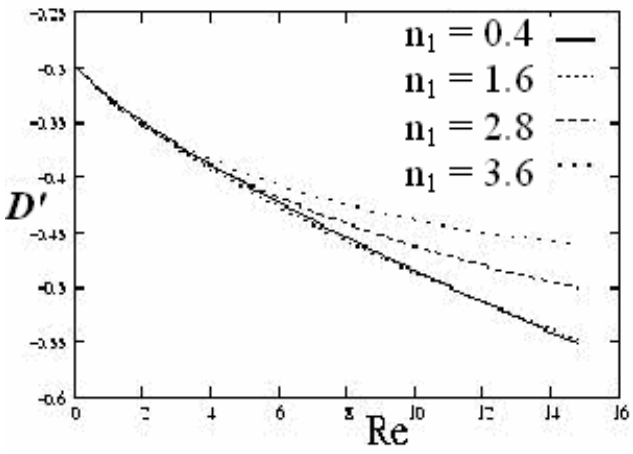

Figure-23. Type B variation of D' with Re.

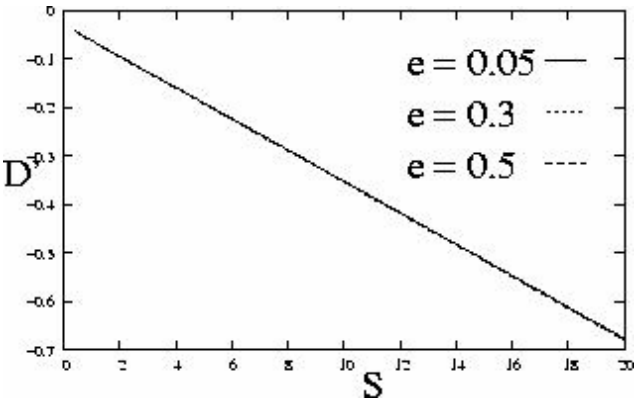

Figure-24. Type A variation of D' with S.

REFERENCES

[1] V.K. Stokes. 1966. Couple stress in fluids. Phys. Fluids. 9: 1709-1715.

[2] V.K. Stokes. 1984. Theories of Fluids with Microstructure. Springer, New York.

[3] G.G. Stokes. 1886. On the effect of rotation of cylinders and spheres about their own axes in increasing the logarithmic decrement of the arc of vibration. Cambridge University Press, England. pp. 207-214.

[4] M.J. Casarella and P.A. Laura. 1969. Drag on oscillating rod with longitudinal and torsional Motion. J. Hydronaut. 3: 180-183.

[5] K.R. Rajagopal. 1983. Longitudinal and Torsional oscillation of a rod in a non-Newtonian fluid. Acta. Mech. 49: 281-285.

[6] H. Ramkissoon and S.R.Majumdar. 1990. Flow due to the longitudinal and torsinal oscillations of a cylinder. ZAMP. 41: 598-603.

[7] H. Ramkissoon, C.V. Easwaran and S.R. Majumdar. 1991. Longitudinal and Torsional oscillation of a rod in a polar fluid. Int. J. Engng. Sci. 29(2): 215-221.

[8] C. Calmelet-Eluhu and D.R. Mazumdar. 1998. Flow of Micropolar fluid through a circular cylinder subject to longitudinal and torsinal oscillations. Mathl. Comput. Modeling. 27: 69-78.

[9] D. Owen and K. Rahaman. 2006. On the flow of an Oldroyd-B liquid through a straight circular tube performing longitudinal and torsional oscillations of different frequencies. Mathematica. 14: 1-9.

[10] A.S. Berman. 1953. Laminar flow in channels with porous walls. J. App. Phys. 24: 1232-1235.

[11] J.R. Sellars. 1955. Laminar flow in channels with porous walls at high suction Reynolds number. J. Appl. Phys. 26: 489-490.

[12] S.W. Yuan. 1956. Further investigation of laminar flow in channels with porous walls. J. Appl. Phys. 27: 267-269.

[13] R.M. Terril, G.M. Shrestha. 1965. Laminar flow through parallel and uniformly porous walls of different permeability. ZAMP. 16: 470-482.

[14] V. M. Soundalgekar and R. N. Aranake. 1974. Effects of couple stresses on the oscillatory flow past an infinite plate with constant suction. Meccanica. pp. 194-197.

[15] N. T. M. Eldabe, A. A. Hassan and Mona A. A. Mohamed. 2003. Effect of Couple Stresses on the MHD of a Non-Newtonian Unsteady Flow between Two Parallel Porous Plates. Z. Naturforsch. 58a. 204-210.

[16] M. Devakar, T.K.V. Iyengar. 2008. Stokes' Problems for an Incompressible Couple Stress Fluid. Nonlinear Analysis: Modeling and Control. 1(2): 181-190.

[17] D. Srinivasacharya, N. Srinivasacharyulu, O. Odelu. 2009. Flow and heat transfer of couple stress fluid in a porous channel with expanding and contracting walls. International Communications in Heat and Mass Transfer. 36: 180-185.

[18] J.V. Ramana Murthy and N.K. Bahali. 2009. Steady flow of micropolar fluid through a circular pipe under a transverse magnetic field with constant suction/injection. Int. J. of Appl. Math and Mech. 5(3): 1-10.

[19] P. Muthu, B.V. Rathish Kumar and Peeyush Chandra. 2008. Peristaltic motion of micropolar fluid in cylindrical tubes: effect of wall properties. Appl. Math. Modeling. 32: 2019-2033.

Appendix

The matrices A_1, X_1, B_1 ; A_2, X_2, B_2; A_3, B_3 and A_4, B_4 defined earlier in the equations (27), (31), (33) and (35) are given by the following expressions.

The coefficient matrix A_1 given in (27) is defined as:

$$A_1=\begin{bmatrix}
0 & t_1 & t_2 & 0 & & & & & & & & & & & \\
t_{1,0} & t_{2,0} & t_{4,0} & t_{5,0} & & & & & & & & & & & \\
 & t_{1,1} & t_{3,1} & t_{4,1} & t_{5,1} & & & & & & & & & & \\
 & & t_{2,2} & t_{3,2} & t_{4,2} & t_{5,2} & & & & & & 0 & & & \\
 & & t_{1,3} & t_{2,3} & t_{3,3} & t_{4,3} & t_{5,3} & & & & & & & & \\
 & & & & & & & & & & & & & & \\
 & & & & & & & t_{1,n-3} & t_{2,n-3} & t_{3,n-3} & t_{4,n-3} & t_{5,n-3} & & & \\
 & & & 0 & & & & & t_{1,n-2} & t_{2,n-2} & t_{3,n-2} & t_{4,n-2} & & & \\
 & & & & & & & & & t_{1,n-1} & t_{2,n-1} & t_{3,n-1} & t_{5,n-1} & & \\
 & & & & & & & & & & t_{1,n} & t_{2,n} & t_{4,n} & t_{5,n} & \\
 & & & & & & & & & & 0 & t_4 & t_5 & 0 &
\end{bmatrix}$$

The solution vector X_1 for velocity v at different points is given by

$X_1 = [v_{-2}, v_{-1}, v_1, v_2, v_3, v_4 \ldots\ldots\ldots v_{n-5}, v_{n-4}, v_{n-3}, v_{n-2}, v_{n-1}, v_n, v_{n+1}, v_{n+2}]^T$

and the vector B_1 for the boundary values is given by

$B_1 = [t_3 v_0, -t_{3,0} v_0, -t_{2,1} v_0, -t_{1,2} v_0, 0\ldots\ldots\ldots\ldots 0, -t_{5,n-2} v_n, -t_{4,n-1} v_n, -t_{3,n} v_n, t_6 v_n]^T$

The matrices A_2, X_2, B_2 defined in equation (31) are as follows. The coefficient matrix A_2 is given by

$$A_2=\begin{bmatrix}
0 & s_1 & s_2 & 0 & & & & & & & & & & & \\
s_{1,0} & s_{2,0} & s_{4,0} & s_{5,0} & & & & & & & & & & & \\
 & s_{1,1} & s_{3,1} & s_{4,1} & s_{5,1} & & & & & & & & & & \\
 & & s_{2,2} & s_{3,2} & s_{4,2} & s_{5,2} & & & & & & 0 & & & \\
 & & s_{1,3} & s_{2,3} & s_{3,3} & s_{4,3} & s_{5,3} & & & & & & & & \\
 & & & & & & & & & & & & & & \\
 & & & & & & & s_{1,n-3} & s_{2,n-3} & s_{3,n-3} & s_{4,n-3} & s_{5,n-3} & & & \\
 & & & 0 & & & & & s_{1,n-2} & s_{2,n-2} & s_{3,n-2} & s_{4,n-2} & & & \\
 & & & & & & & & & s_{1,n-1} & s_{2,n-1} & s_{3,n-1} & s_{5,n-1} & & \\
 & & & & & & & & & & s_{1,n} & s_{2,n} & s_{4,n} & s_{5,n} & \\
 & & & & & & & & & & 0 & s_3 & s_4 & 0 &
\end{bmatrix}$$

The solution vector X_2 for velocity w at different points is given by

$X_2 = [w_{-2}, w_{-1}, w_1, w_2, w_3, w_4, w_{5..} \ldots\ldots\ldots w_{n-5}, w_{n-4}, w_{n-3}, w_{n-2}, w_{n-1}, w_n, w_{n+1}, w_{n+2}]$ T

and the vector B_2 for the boundary values is given by

$B_2 = [2r_0 w_0, -s_{3,0} w_0, -s_{2,1} w_0, -s_{1,2} w_0, 0\ldots\ldots\ldots 0, -s_{5,n-2} w_n, -s_{4,n-1} w_n, -s_{3,n} w_n, 2r_n w_n]^T$

The coefficient matrix A_3 defined in equation (33) is given by

$$A_3=\begin{bmatrix}
0 & 1 & -1 & 0 & & & & & & & & & & & \\
t_{1,0} & t_{2,0} & t_{4,0} & t_{5,0} & & & & & & & & & & & \\
 & t_{1,1} & t_{3,1} & t_{4,1} & t_{5,1} & & & & & & & & & & \\
 & & t_{2,2} & t_{3,2} & t_{4,2} & t_{5,2} & & & & & & 0 & & & \\
 & & t_{1,3} & t_{2,3} & t_{3,3} & t_{4,3} & t_{5,3} & & & & & & & & \\
 & & & & & & & & & & & & & & \\
 & & & & & & & t_{1,n-3} & t_{2,n-3} & t_{3,n-3} & t_{4,n-3} & t_{5,n-3} & & & \\
 & & & 0 & & & & & t_{1,n-2} & t_{2,n-2} & t_{3,n-2} & t_{4,n-2} & & & \\
 & & & & & & & & & t_{1,n-1} & t_{2,n-1} & t_{3,n-1} & t_{5,n-1} & & \\
 & & & & & & & & & & t_{1,n} & t_{2,n} & t_{4,n} & t_{5,n} & \\
 & & & & & & & & & & 0 & 1 & -1 & 0 &
\end{bmatrix}$$

and the vector B_3 for the boundary values is given by

$$B_3 = [(2h/r_0)v_0, -t_{3,0}\, v_0, -t_{2,1}\, v_0, -t_{1,2}\, v_0, 0, \ldots., 0, -t_{5,n-2}\, v_n, -t_{4,n-1}\, v_n, -t_{3,n}\, v_n, (2h/r_n)v_n]^T$$

The coefficient matrix A_4 defined in equation (35) is given by

$$A_4=\begin{bmatrix}
0 & 1 & -1 & 0 & & & & & & & & & & & \\
s_{1,0} & s_{2,0} & s_{4,0} & s_{5,0} & & & & & & & & & & & \\
 & s_{1,1} & s_{3,1} & s_{4,1} & s_{5,1} & & & & & & & & & & \\
 & & s_{2,2} & s_{3,2} & s_{4,2} & s_{5,2} & & & & & & 0 & & & \\
 & & s_{1,3} & s_{2,3} & s_{3,3} & s_{4,3} & s_{5,3} & & & & & & & & \\
 & & & & & & & & & & & & & & \\
 & & & & & & & s_{1,n-3} & s_{2,n-3} & s_{3,n-3} & s_{4,n-3} & s_{5,n-3} & & & \\
 & & & 0 & & & & & s_{1,n-2} & s_{2,n-2} & s_{3,n-2} & s_{4,n-2} & & & \\
 & & & & & & & & & s_{1,n-1} & s_{2,n-1} & s_{3,n-1} & s_{5,n-1} & & \\
 & & & & & & & & & & s_{1,n} & s_{2,n} & s_{4,n} & s_{5,n} & \\
 & & & & & & & & & & 0 & 1 & -1 & 0 &
\end{bmatrix}$$

and the vector B_4 for the boundary values is given by

$$B_4 = [4\sigma_1 h, -s_{3,0}\, w_0, -s_{2,1}\, w_0, -s_{1,2}\, w_0, 0,\ldots\ldots\ldots,0, -s_{5,n-2}\ w_n, -s_{4,n-1}\, w_n, -s_{3,n}\, w_n, 0]^T$$